

The alkenone–CO₂ proxy and ancient atmospheric carbon dioxide

BY MARK PAGANI†

*Natural Resource Ecology Laboratory, Colorado State University,
Fort Collins, CO 80523, USA*

Published online 18 March 2002

Cenozoic climates have varied across a variety of time-scales, including slow, unidirectional change over tens of millions of years, as well as severe, geologically abrupt shifts in Earth's climatic state. Establishing the history of atmospheric carbon dioxide is critical in prioritizing the factors responsible for past climatic events, and integral in positioning future climate change within a geological context. One approach in this pursuit uses the stable carbon isotopic composition of marine organic molecules known as alkenones. The following report represents a summary of the factors affecting alkenone carbon isotopic compositions, the underlying assumptions and accuracy of short- and long-term CO₂ records established from these sedimentary molecules, and their implications for the controls on the evolution of Cenozoic climates.

Keywords: atmospheric carbon dioxide; alkenones; carbon isotope ratios; Cenozoic

1. Introduction

The identification of patterns and forcing mechanisms of ancient climates is a fundamental component of Earth system research. In general, the primary mechanisms driving long-term Cenozoic climate variability include orogenesis (Ruddiman *et al.* 1989, 1997), alterations in ocean circulation driven by relatively subtle changes in surface water density, and/or long-term, tectonically induced changes in basinal topography (Kennett 1977) and variations in atmospheric 'greenhouse' gases, notably carbon dioxide and methane concentrations (Berner & Kothavala 2001). Of these factors, the evolution of the partial pressure of atmospheric carbon dioxide is widely credited for the expression of long-term climate change over the past 65 Myr (Raymo *et al.* 1988; Cerling *et al.* 1997). However, other compelling arguments have been presented that call on the gradual, tectonically mediated reorganization of ocean circulation as the principal mechanism responsible for the history of Cenozoic ice accumulation (Kennett 1977; Keigwin 1982).

In lieu of direct measurements, palaeoatmospheric carbon dioxide concentrations and trends have been established in a variety of ways (Arthur *et al.* 1985, 1991; Vincent & Berger 1985; Compton *et al.* 1990; Cerling *et al.* 1997; Raymo 1994; Freeman & Hayes 1992; Pagani *et al.* 1999a; Pearson & Palmer 2000; van der Burg *et al.* 1993). One approach that shows great promise in establishing an accurate

† Present address: Department of Geology and Geophysics, Yale University, New Haven, CT 06520, USA.

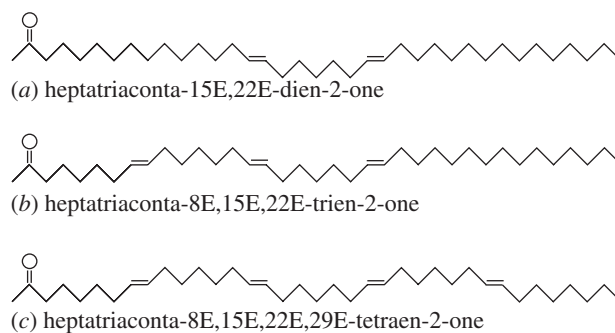


Figure 1. C₃₇ unsaturated methyl ketones (Brassell *et al.* 1986; Rechka & Maxwell 1987). (a) Diunsaturated alkenone; (b) triunsaturated alkenones; (c) tetraunsaturated alkenones.

history of pCO₂ uses the stable carbon isotopic composition of sedimentary organic molecules known as alkenones. Alkenones are long-chained (C₃₇–C₃₉) unsaturated ethyl and methyl ketones primarily synthesized within the ocean mixed layer by a few species of haptophyte algae (Conte *et al.* 1994). Of these molecular forms, C₃₇ diunsaturated alkenones (figure 1a) have been extensively studied in both the laboratory and the field (Bidigare *et al.* 1997; Popp *et al.* 1998), and commonly applied in the evaluation of ancient pCO₂ (Jasper & Hayes 1990; Jasper *et al.* 1994; Pagani *et al.* 1999a, b).

Common in surface marine sediments, alkenones are found throughout Palaeogene and Neogene deposits, with the oldest occurrence currently identified in a Mid-Albian black shale (Farrimond *et al.* 1986). The dominant alkenone producers in modern oceans include *Emiliania huxleyi* and *Gephyrocapsa oceanica*. However, *E. huxleyi* is known from the Late Pleistocene to the present (McIntyre 1970), whereas *G. oceanica* extends to the Pliocene (Hay 1977). Examination of older sediments containing both alkenones and nannofossils has narrowed the probable source of alkenones in the sedimentary record to microalgae within the family Noelaerhabdaceae (Marlowe *et al.* 1990; Volkman 2000).

Alkenones, and various other lipids, are commonly separated from bulk organic matter using traditional adsorption chromatographic techniques. In this process, the total lipid extract is passed through a column packed with solid particles (such as silica) using a series of increasingly polar organic solvents. Adsorption of the solute onto the surface of the particles, and equilibration between the adsorbed state and solution, leads to the partitioning of molecules into compound classes. Once alkenones are identified by gas chromatography–mass spectrometry (GC-MS), or by comparison of elution times with a known standard, compound-specific carbon isotope analyses are performed using a gas chromatograph–combustion system interfaced to an isotope-ratio-monitoring mass spectrometer (GC-IRMS) (Merritt *et al.* 1995).

2. Variables affecting the stable isotopic composition of marine algae

(a) Evidence from culture experiments

The alkenone–CO₂ method is founded on the observation that the stable carbon-isotope composition of marine algae ($\delta^{13}\text{C}_{\text{org}}$) contains information that is relevant to the concentration of dissolved carbon dioxide during algal production (Wong &

Sackett 1978; Rau *et al.* 1989, 1992). However, other factors including cellular growth rate (Rau *et al.* 1992; Francois *et al.* 1993; Laws *et al.* 1995; Bidigare *et al.* 1997), cell geometry (Popp *et al.* 1998), as well as the mechanisms used to supply and transport inorganic carbon to the site of carbon fixation, substantially affect algal carbon isotopic compositions. For example, many microalgae appear to have the ability to actively increase both intercellular and extracellular CO₂ concentrations (Sharkey & Berry 1985; Falkowski 1991; Raven & Johnston 1991), and employ a variety of enzymes during carbon fixation (see Goericke *et al.* 1994). These variables can greatly affect the relative expression of $\delta^{13}\text{C}_{\text{org}}$ between different classes of microalgae. As a result, not all algae, or their molecular components, can be used as reliable CO₂ tracers.

Two criteria need to be satisfied for $\delta^{13}\text{C}_{\text{org}}$ to act as a potential CO_{2aq} proxy:

- (1) the inorganic carbon used during carbon fixation is in the form of aqueous carbon dioxide (CO_{2aq}), and
- (2) the supply of CO_{2aq} used during photosynthesis arrives from the ambient environment to the site of carboxylation by simple diffusion.

If these conditions are realized, then the magnitude of total carbon isotope discrimination, which occurs during photosynthesis (ε_p) can be expressed as a function of the isotope fractionations associated with carbon transport and fixation, as well as the extracellular and intercellular concentrations of CO_{2aq} (Farquhar *et al.* 1982):

$$\varepsilon_p = \varepsilon_t + (\varepsilon_f - \varepsilon_t)(C_i/C_e), \quad (2.1)$$

where ε_f and ε_t are constants representing the carbon isotope fractionations associated with carbon fixation and diffusive transport, and C_e and C_i are the extracellular and intercellular concentrations of CO₂, respectively.

Initial research focused on the influence of C_e on $\delta^{13}\text{C}_{\text{org}}$ (Degens *et al.* 1968; Wong & Sackett 1978). More recently it has become evident that the intercellular pool of carbon dioxide (C_i) exerts considerable control over ε_p . Because quantification of intercellular CO₂ is difficult and generally elusive, attempts have been made to recast equation (2.1) in terms of the physiological variables that exert control over C_i . If one accepts that the specific growth rate (μ) of an algal cell (i.e. the net flux of CO_{2aq} divided by the carbon per cell) is related to C_i by the relationship (Rau *et al.* 1992; Francois *et al.* 1993; Laws *et al.* 1995, 1997)

$$\mu = \frac{k_1 C_e - k_2 C_i}{C}, \quad (2.2)$$

where C is the carbon content of the cell, and k_1 and k_2 are rate constants for the diffusion of CO_{2aq} into and out of the cell; in which case, equation (2.1) can be recast as

$$\varepsilon_p = \varepsilon_t + (\varepsilon_f - \varepsilon_t) \left(1 - \frac{\mu C}{k C_e} \right). \quad (2.3)$$

This formulation reasonably assumes that for a diffusive model of carbon uptake, the resistance to diffusion of CO_{2aq} into and out of the cell is equivalent (i.e. $k_1 = k_2 = k$). It follows that the rate of diffusion for CO_{2aq} will be proportional to the permeability of the cell membrane, which is arguably related to cellular surface area (Laws *et al.*

1995, 1997). Furthermore, one anticipates that the carbon content of the cell will be proportional to the biovolume of the micro-organism (Verity *et al.* 1993; Popp *et al.* 1998).

Further model simplifications are applied in field-based research, where physiological parameters are difficult to quantify. For these data, equation (2.3) is commonly reduced to

$$\varepsilon_p = \varepsilon_f - (b/C_e), \quad (2.4)$$

where b represents an integration of all the physiological variables, such as growth rate and cell geometry, affecting the total carbon isotope fractionation during photosynthesis (Jasper *et al.* 1994; Bidigare *et al.* 1997).

Chemostat incubations for the alkenone-producing haptophyte algae *Emiliania huxleyi* (Bidigare *et al.* 1997) and diatoms *Phaeodactylum tricorutum* (Laws *et al.* 1997) and *Porosira glacialis* (Popp *et al.* 1998) provide supporting evidence for the theoretical model described in equation (2.3) (figure 2a). These three experiments, performed under nitrate-limited conditions, demonstrate that ε_p varies linearly in respect to the ratio of $\mu/\text{CO}_{2\text{aq}}$, each with different slopes and identical y -intercepts (*ca.* 25‰, see below). The y -intercept represents the value of ε_f as $\mu/\text{CO}_{2\text{aq}}$ approaches zero (see equation (2.3)). Moreover, differences in slopes can be normalized by accounting for differences in cell geometries, specifically the ratio of volume to surface area (Popp *et al.* 1998) (figure 2b). Although these experimental results are consistent with a diffusive model of carbon uptake, linear relationships between ε_p and $\mu/\text{CO}_{2\text{aq}}$ can also be explained by models incorporating the effects of active carbon uptake (Popp *et al.* 1998).

Active carbon uptake and/or other carbon-concentrating mechanisms have been detected in various algae. Laws *et al.* (1997) demonstrated that under extremely low $[\text{CO}_{2\text{aq}}]$ (less than $4 \mu\text{mol kg}^{-1}$) the relationship between ε_p and $\mu/\text{CO}_{2\text{aq}}$ for *P. tricorutum* sharply deviates from linearity (figure 2c). Nonlinearity is consistent with either active uptake of inorganic carbon or CO_2 augmentation through the extracellular enzymatic conversion of HCO_3^- to $\text{CO}_{2\text{aq}}$ (Laws *et al.* 1997).

It is possible, however, that different growth and environmental conditions trigger different carbon uptake pathways, as well as carbon isotopic responses (Laws *et al.* 2000). For example, strains of *E. huxleyi*, *P. tricorutum* and *P. glacialis* grown in dilute batch cultures, under nitrate-replete conditions and varying light:dark cycles, demonstrate that although ε_p varies with respect to $\text{CO}_{2\text{aq}}$ and $\mu/\text{CO}_{2\text{aq}}$, these relationships differ from those established in nutrient-limited, predominantly continuous-light, chemostat incubations (Burkhardt *et al.* 1999; Riebesell *et al.* 2000). Relative to chemostat cultures, dilute batch cultures result in substantially lower absolute ε_p values, and different, as well as nonlinear, species-specific slopes for ε_p versus $\mu/\text{CO}_{2\text{aq}}$ (figure 3).

In palaeo- CO_2 reconstructions, the value of ε_f (carbon isotope fractionation factor attributed to carboxylation) applied becomes increasingly important as the magnitude of ε_p increases. Although recent chemostat experiments suggest that a value of 25‰ is an appropriate value for ε_f for a variety of microalgae (figure 2a), a wider range is possible. For example, a value of 29‰ is widely accepted for the *in vitro* fractionation factor of Rubisco (ribulose-1,5-biphosphate carboxylase/oxygenase) with respect to aqueous CO_2 (Roeske & O'Leary 1984; Raven & Johnston 1991). However, a smaller *in situ* fractionation associated with carbon fixation in algae is commonly observed and generally attributed to the effects of other enzymes, such as

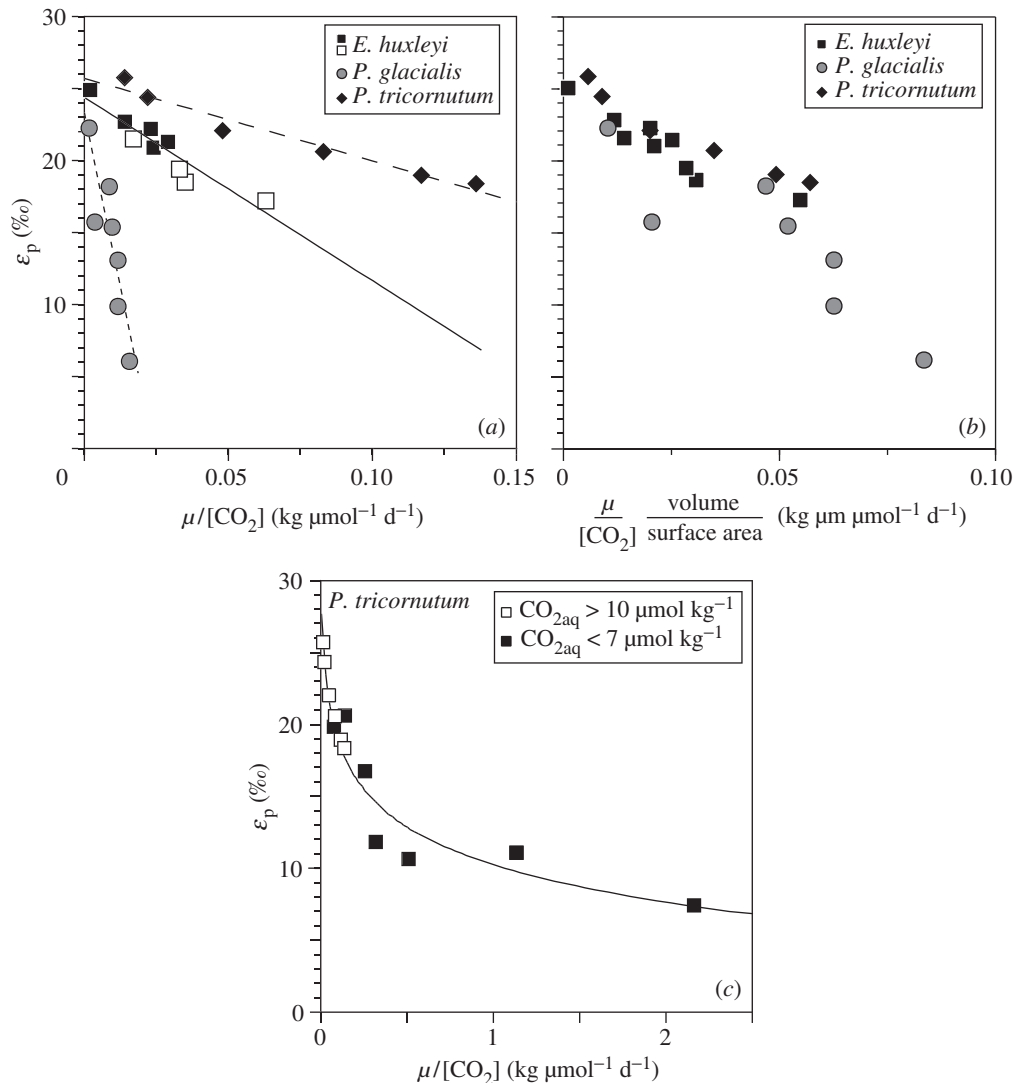


Figure 2. Comparison of ϵ_p with $\mu/[\text{CO}_{2\text{aq}}]$. (a) Chemostat incubations (from Popp *et al.* 1998). All experiments were conducted under nitrate-limited, continuous-light conditions, except for *P. tricorunutm*, which includes both continuous-light and 12 h : 12 h light:dark cycles. Diamonds, *P. tricorunutm* (Laws *et al.* 1995); squares (calcifying, closed squares; non-calcifying, open squares) *E. huxleyi* (Bidigare *et al.* 1997); circles, *P. glacialis* (Popp *et al.* 1998). (b) Comparison of ϵ_p with $(\mu/[\text{CO}_{2\text{aq}}])$ (volume/surface area) (from Popp *et al.* 1998). (c) Effect of low $[\text{CO}_{2\text{aq}}]$ on *P. tricorunutm*. Closed squares, greater than $10 \mu\text{mol kg}^{-1}$; open squares, less than $7 \mu\text{mol kg}^{-1}$ (Laws *et al.* 1995, 1997).

the β -carboxylase, phosphoenolpyruvate-carboxylase (Farquhar & Richards 1984). Goericke *et al.* (1994) calculated a range of 25–28‰ for ϵ_f in algae with C₃-type metabolisms, considering a 2–10% contribution of β -carboxylation to the total carboxylation. Given our limited knowledge of ancient algal physiologies, this broader, more conservative range of ϵ_f should be applied in palaeo-pCO₂ reconstructions.

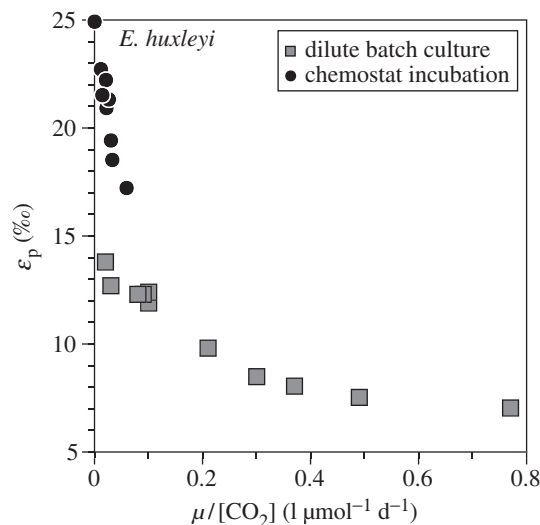


Figure 3. Comparison of ϵ_p with $\mu/[CO_{2aq}]$ from chemostat and dilute batch cultures of *E. huxleyi* (from Riebesell *et al.* 2000). Circles, chemostat incubation (Bidigare *et al.* 1997), conducted under nitrate-limited, continuous-light conditions. Squares, dilute batch cultures (Riebesell *et al.* 2000), performed under nitrate-saturated, 16 h : 8 h light:dark regime.

In summary, the stable carbon isotopic composition of marine algae is a function of the carbon isotopic composition of inorganic dissolved carbon, surface-water $[CO_{2aq}]$, cellular growth rate, cellular geometry and possibly irradiance and nitrate concentration (Riebesell *et al.* 2000; Eek *et al.* 1999). Clearly, care must be taken in the interpretation of $\delta^{13}C_{org}$. Furthermore, bulk sedimentary marine organic carbon potentially contains significant contributions from terrestrial sources (Pagani *et al.* 2000b). Thus, when establishing isotopic records from bulk sedimentary organic matter, one can only be confident of analysing carbon derived exclusively from marine organic matter, free from biases associated with selective preservation, by using molecular markers from known marine sources (Hayes *et al.* 1990; Freeman *et al.* 1990). Therefore, by restricting analysis to alkenone carbon isotope chemistry, and, by extension, the limited population of alkenone-producing organisms, the effect of cell geometry and other physiological effects are arguably mitigated. If variation in growth rate is constrained, alkenone ϵ_p values presumably provide information that is specific to surface-water $[CO_{2aq}]$ and pCO_2 .

It is important to recognize that the carbon isotopic composition of alkenones is distinct from bulk haptophyte organic matter due to additional isotopic fractionations that occur during lipid biosynthesis. Therefore, a correction is applied to alkenone $\delta^{13}C$ in order to establish ϵ_p values that represent the isotopic difference between the algal biomass and the inorganic carbon used during photosynthesis. Cultures performed under various experimental conditions indicate that the isotopic difference between alkenone and bulk $\delta^{13}C$ ($\Delta\delta$) has a narrow range (*ca.* $-4.2 \pm 1\%$) for two alkenone-producing algae (see Laws *et al.* (2000) for a review). Given the available data, $\Delta\delta$ is assumed invariant in palaeo- pCO_2 studies (Pagani *et al.* 1999a). However, it is possible that secular changes in the relative ratio of proteins, carbohydrates and lipids in alkenone-producing organisms can impact the value of $\Delta\delta$.

(Riebesell *et al.* 2000). Given the experimental range for $\Delta\delta$, such variability will have little impact on palaeo-pCO₂ interpretations when the value of ε_p is low, but becomes increasingly important as ε_p approaches maximum theoretical values.

Finally, changes in the partial pressure of atmospheric oxygen (pO_2) can also play a role in the relative magnitude of ε_p over geologic time. Recent experiments indicate that rather large changes in pO_2 can potentially impact the $\delta^{13}C$ of marine algae (Berner *et al.* 2000). This effect is potentially driven by an increase in photorespiration rates due to the oxygenase function of Rubisco, leading to an increase in fixation rates of ¹³C-depleted respired CO₂. Although these results point to an additional control on the $\delta^{13}C$ of marine algae, it is unlikely to alter the interpretation of Cenozoic ε_p trends because the change in isotopic fractionation attributable to large variations in pO_2 (ca. –1.4‰ for *P. tricornutum*) under moderately low CO₂ conditions is relatively small.

A more comprehensive review of the issues discussed above can be found in Laws *et al.* (2000).

(b) Data from natural haptophyte populations

Extensive alkenone carbon isotopic measurements from natural haptophyte populations have been performed across an array of oceanic environments (Bidigare *et al.* 1997, 1999; Popp *et al.* 1999; Eek *et al.* 1999; Laws *et al.* 2000). These data provide evidence for a robust relationship between the physiological-dependent term b (see equation (2.4)) and the concentration of reactive soluble phosphate (figure 4). Given our understanding of the factors controlling $\delta^{13}C_{org}$, it is likely that differences in relative growth rates are responsible for this relationship. Although phosphate is a major limiting nutrient, it is unlikely that $[PO_4^{3-}]$ alone is responsible for the variability in growth rate inferred from variation in b . Instead, it is assumed that the availability of one or more trace elements, which display phosphate-like distributions in the ocean (i.e. Se, Co, Ni), is ultimately influencing the growth characteristics of these populations (see Bidigare *et al.* 1997; Laws *et al.* 2000 and references cited therein).

An alternative explanation is that the apparent correlation of b with $[PO_4^{3-}]$ is the result of chemical oceanography, and not growth-related factors. Because the term b is a function of CO₂ (i.e. $b = (\varepsilon_f - \varepsilon_p)CO_2$), the relationship displayed in figure 4 could ultimately reflect a b versus $[CO_{2aq}]$ correlation through the natural association of phosphate with dissolved carbon dioxide. Bidigare *et al.* (1997) explored this possibility in their original dataset ($n = 39$) and found that the correlation between $[PO_4^{3-}]$ and $[CO_{2aq}]$ ($r^2 = 0.65$) was poor relative to that of b versus $[PO_4^{3-}]$ ($r^2 = 0.95$). On this basis, they concluded that a ε_p – $[PO_4^{3-}]$ relationship was robust. However, the most recent dataset ($n = 109$) reveals a similarly high correlation between $[PO_4^{3-}]$ and $[CO_{2aq}]$ ($r^2 = 0.80$) and b versus $[PO_4^{3-}]$ ($r^2 = 0.78$) (figure 5). Nonetheless, given the apparent association of $[PO_4^{3-}]$ with $[CO_{2aq}]$, there is no correlation when ε_p is compared with $1/[CO_{2aq}]$ (see equation (2.3)), while a clearer relationship between ε_p and $[PO_4^{3-}]$ ($r^2 = 0.23$) is evident (figure 6). Popp *et al.* (1999) emphasized this conclusion by suggesting that the effect of $[PO_4^{3-}]$ on ε_p is readily apparent if one restricts analysis to samples with a relatively invariant range of $[CO_{2aq}]$ (i.e. 12–16.5 $\mu\text{mol kg}^{-1}$). Moreover, correlation of ε_p with $[PO_4^{3-}]$ improves when $[PO_4^{3-}]$ is normalized to $[CO_{2aq}]$ (figure 7).

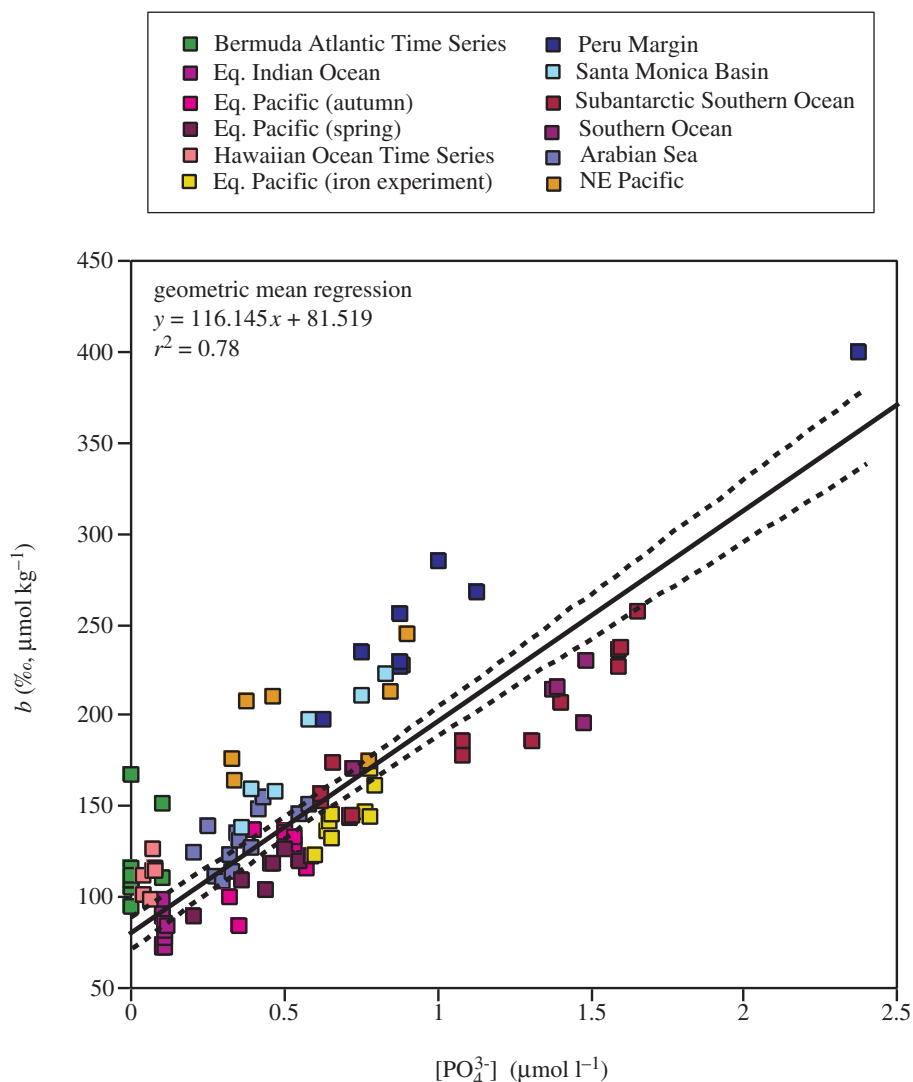


Figure 4. Compilation of b versus soluble phosphate for natural haptophyte populations (Bidigare *et al.* 1997, 1999; Popp *et al.* 1999; Eek *et al.* 1999; Laws *et al.* 2000). Values for b are calculated using a value of 25‰ for ε_f . The solid line represents geometric mean regression. Dotted lines reflect 95% confidence intervals. Note: the term b is related to ε_p through equation (2.4).

In an attempt to explain data that deviate from the global b versus $[\text{PO}_4^{3-}]$ regression, Eek *et al.* (1999) argued that the ε_p versus $[\text{PO}_4^{3-}]/[\text{CO}_{2\text{aq}}]$ relationship is robust when the concentration of $\text{NO}_3 + \text{NO}_2$ ($[N]$) is greater than zero, but fails when $[N] = 0$. While data from some low- $[N]$ environments (i.e. Hawaiian Ocean Time Series, Bermuda Atlantic Time Series) lend support to this supposition, low- $[N]$ data from the Equatorial Indian Ocean and the Arabian Sea do not. To date, the totality of factors responsible for the scatter in the available data for both ε_p versus $[\text{PO}_4^{3-}]/[\text{CO}_{2\text{aq}}]$ and b versus $[\text{PO}_4^{3-}]$ remains elusive.

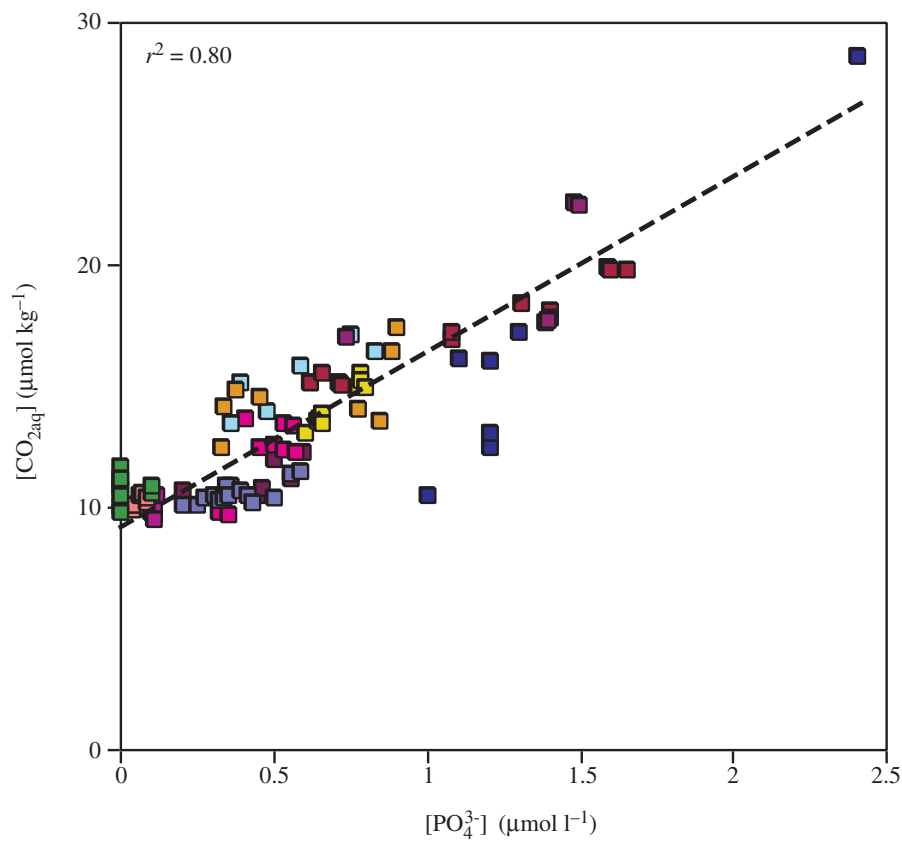


Figure 5. Plot of $[\text{CO}_{2\text{aq}}]$ versus $[\text{PO}_4^{3-}]$. The dashed line denotes geometric mean regression.

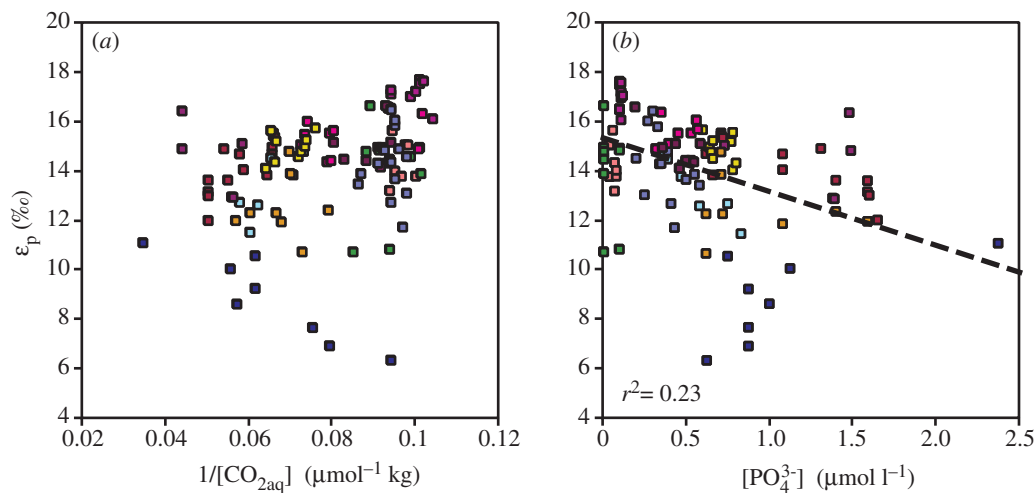


Figure 6. (a) Plot of ϵ_p versus $1/[\text{CO}_{2\text{aq}}]$. (b) Plot of ϵ_p versus $[\text{PO}_4^{3-}]$. The dashed line denotes geometric mean regression.

Clearly, if distinct regional differences exist between alkenone carbon isotope compositions and ocean chemistry, it questions the validity of a global ε_p -CO₂ calibration based on [PO₄³⁻]. Furthermore, the results of culture experiments raise critical questions regarding the effects of light- versus nutrient-limited growth, as well as the validity of the diffusion model of carbon uptake (equations (2.1), (2.3)). For example, the depth of haptophyte production within subtropical gyres may exceed 100 m, placing a portion of alkenone synthesis within the limits of the photic zone (Ohkouchi *et al.* 1999). If light-limited growth greatly affects alkenone-derived ε_p values in the natural environment, one would anticipate large errors between alkenone-based [CO_{2aq}] and water-column [CO_{2aq}] across well-stratified, nutrient-poor, subtropical regimes.

3. Accuracy of alkenone-based CO₂ records

In an effort to test the precision of the alkenone-CO₂ approach, Pagani *et al.* (2002) established pre-industrial water-column [CO_{2aq}] from sedimentary alkenone $\delta^{13}\text{C}$ values across a North Pacific transect (along 175° E from 45° N to 15° S) (figure 8). Sedimentary alkenone-based CO_{2aq} estimates ([CO_{2aq}]_{alk}) were established by first identifying the depth of alkenone production at each site as defined by U₃₇^{K'} temperature estimates (Ohkouchi *et al.* 1999) and seasonal temperature-depth relationships established by the Northwest Pacific Carbon Cycle Study (Tsubota *et al.* 1999). The production depths inferred by these records were then used to designate $\delta^{13}\text{C}_{\text{CO}_{2\text{aq}}}$ values and [PO₄³⁻] required in the calculation of ε_p and [CO_{2aq}]_{alk}.

The results of this work provide critical evidence supporting the efficacy of the alkenone CO₂ approach. Pre-industrial alkenone-based [CO_{2aq}] across the subtropics (between 40° N and 20° N) deviate from water-column concentrations consistent with a 30% anthropogenic increase in pCO₂ over the past 150 years. When the effects of anthropogenic [CO_{2aq}] are removed from the modern signal, alkenone CO_{2aq} estimates accurately reproduce pre-industrial water-column concentrations with the majority of reconstructed [CO_{2aq}] falling within 20% of modelled pre-industrial water-column concentrations (figure 9).

The relative accuracy of the alkenone-CO₂ method across the subtropics, where the lowest [CO_{2aq}] and potentially the deepest production depths occur (Ohkouchi *et al.* 1999) suggests that either the occurrence of light-limited growth and active carbon uptake are negligible or that these processes have negligible effects on carbon isotopic compositions of haptophytes in the natural environment. In either case, these results demonstrate that the alkenone approach can be used to accurately reconstruct water-column CO₂ when phosphate concentrations and temperatures are well constrained.

4. Ancient alkenone-based pCO₂ records

(a) Neogene research

The alkenone methodology has been applied to evaluate palaeo-oceanographic dynamics and surface-water [CO_{2aq}] during the Pleistocene (Jasper & Hayes 1990; Jasper *et al.* 1994), Late Quaternary surface-water pCO₂ in the South Atlantic (Andersen *et al.* 1999), and global Miocene pCO₂ trends (Pagani *et al.* 1999a, b).

In general, ancient ε_p records are established by measuring the carbon isotopic composition of diunsaturated alkenones and coeval near-surface-dwelling planktonic foraminifera. The $\delta^{13}\text{C}$ values of foraminiferal carbonate are then used to estimate the $\delta^{13}\text{C}$ of $\text{CO}_{2\text{aq}}$ in equilibrium with calcite. Site selection for Miocene research focused on several low-growth, oligotrophic environments. In this way, the range of phosphate concentrations available for algal production was narrowed, allowing for more accurate $[\text{CO}_{2\text{aq}}]$ estimates. Furthermore, the low air-to-sea gas disequilibrium characteristic of these oceanic settings reduces uncertainty in the calculation of pCO_2 . Miocene ε_p records from four ocean localities are shown in figure 10. When compared with modern ε_p values, Miocene values fall on the low end of the spectrum suggesting either the untenable conclusion that haptophyte growth rates were anomalously high in low productive waters or that CO_2 concentrations were similar to or, more likely, below modern levels (figure 11).

Temporal differences in the pattern of Miocene ε_p values between sites can be explained in terms of regional differences in algal growth rates. It follows that sustained changes in regional growth rates imply substantial changes in physical oceanographic conditions. For example, rapid change in ε_p values (*ca.* 20 Ma) at Site 516 in the Southwest Atlantic was interpreted as reflecting substantial changes in surface-water nutrient concentrations. Arguments were presented that linked the timing of these changes to the opening of the Drake Passage, the onset of deep-water flow through the passage, and subsequent invigoration of the Antarctic Circumpolar Current and Antarctic Intermediate Water production (Pagani *et al.* 2000a).

Miocene atmospheric carbon dioxide concentrations were estimated (figure 12) from ε_p values by applying phosphate concentrations typical of these environments, and temperatures derived from $\delta^{18}\text{O}$ values from shallow-dwelling foraminifera. The results suggest that during much of the Miocene, the maximum pCO_2 (less than 290 ppmv) was far lower than modern levels, falling within a range similar to Pleistocene glacial/interglacial concentrations (Pagani *et al.* 1999a). These results are further supported by a recent convergence of CO_2 estimates derived from distinctly different approaches (Pearson & Palmer 2000; van der Burg *et al.* 1993; Royer *et al.* 2001). Moreover, recent efforts have provided new data that extend ε_p records from the Miocene into the Pleistocene (M. Pagani, K. H. Freeman & M. A. Arthur 2002, unpublished data). The magnitude of Pliocene/Pleistocene ε_p values are indistinguishable from Miocene values (table 1, figure 10), providing evidence that the factors controlling the isotopic expression of alkenones (i.e. CO_2 , growth rate) at these localities have remained remarkably stable for the past 25 Myr.

Low Neogene CO_2 concentrations are particularly surprising in light of the climatic and ecological events that occurred during this time. The early Miocene is characterized as an interval of expansive high-latitude warmth, leading to deep-water temperatures *ca.* 6 °C warmer than today (Shackleton & Kennett 1975; Savin *et al.* 1975). In contrast, the middle Miocene is known for rapid high-latitude cooling and East Antarctic ice-sheet expansion (Shackleton & Kennett 1975; Miller *et al.* 1987; Wright *et al.* 1992; Flower & Kennett 1993). Although the late Miocene is not recognized for distinctive changes in global climates, it is acknowledged as a period of important ecological change. Carbon isotopic evidence from palaeosol carbonates and fossil tooth enamel support a rapid, predominantly low-latitude expansion of C_4 grasses between *ca.* 8 and 4 Ma (Cerling *et al.* 1997). This floral shift is argued to have resulted from a decline in carbon dioxide across a critical threshold (*ca.* 500–

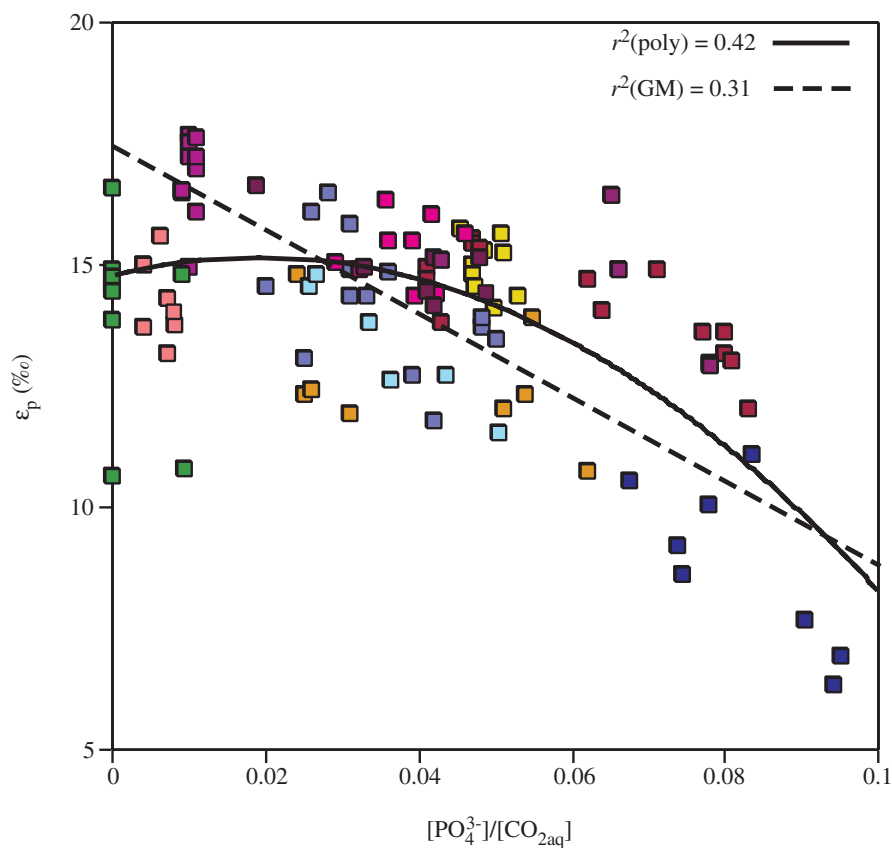


Figure 7. Plot of ε_p versus $[\text{PO}_4^{3-}]/[\text{CO}_{2\text{aq}}]$. The dashed line represents geometric regression ($r^2 = 0.31$). The solid line represents polynomial regression ($r^2 = 0.42$).

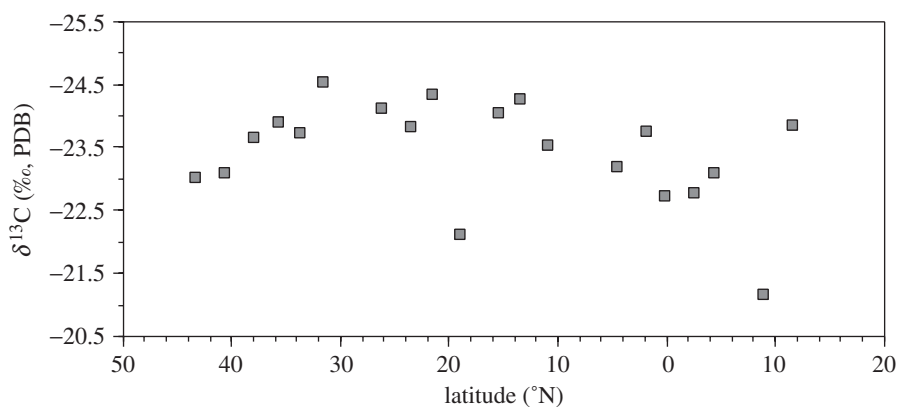


Figure 8. Stable carbon isotopic compositions of Holocene-age, diunsaturated alkenones from a North Pacific transect (175°E) (Pagani *et al.* 2002). Samples were collected with a box corer during the RV *Hakurei Maru* cruises in 1992/1993, frozen, and subsequently analysed for $\text{U}_{37}^{K'}$ temperature values (Ohkouchi *et al.* 1999).

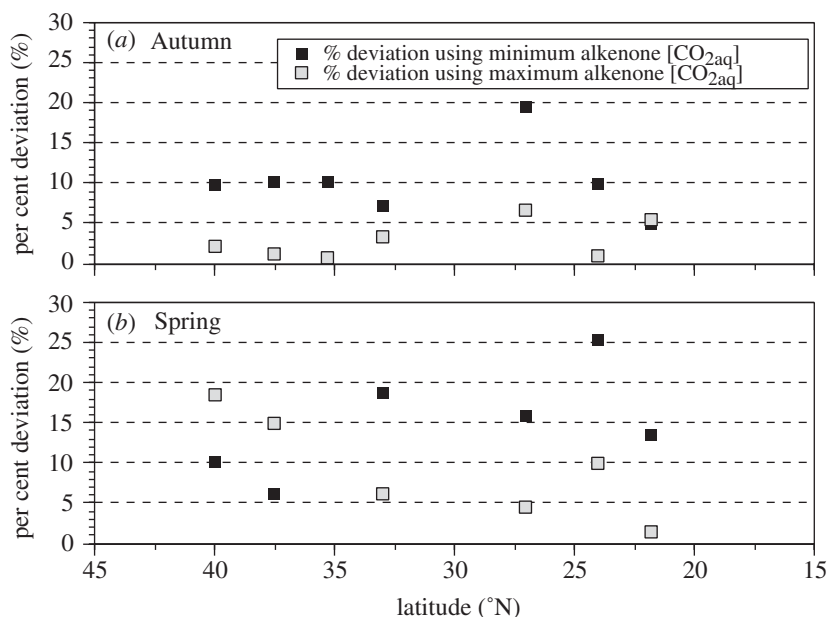


Figure 9. Per cent deviation of alkenone-based $[\text{CO}_{2\text{aq}}]$ from modelled pre-industrial $[\text{CO}_{2\text{aq}}]$. (a) Per cent deviation assuming that haptophyte production occurred in the autumn (August and September). (b) Per cent deviation assuming that haptophyte production occurred in the spring (April, May and June). Alkenone-based $[\text{CO}_{2\text{aq}}]$ were calculated from reconstructed ε_{p} values. $\varepsilon_{\text{p}} = [(\delta\text{C}_{\text{CO}_{2\text{aq}}} + 1000)/(\delta_{\text{org}} + 1000) - 1]10^3$, where $\delta_{\text{org}} \approx \delta^{13}\text{C}_{\text{alk}} + 4$ and $\delta\text{C}_{\text{CO}_{2\text{aq}}}$ represents $\delta^{13}\text{C}$ values of pre-industrial $\text{CO}_{2\text{aq}}$. Pre-industrial $\delta\text{C}_{\text{CO}_{2\text{aq}}}$ values were calculated from pre-industrial δ_{DIC} by adjusting modern δ_{DIC} values by *ca.* 1‰ between 20° and 40° N (Lynch-Stieglitz *et al.* 1995). Modern δ_{DIC} values were established using data from the World Ocean Circulation Experiment (WOCE P13) and Kroopnick (1985). Maximum alkenone-based $[\text{CO}_{2\text{aq}}]$ calculated using an $\varepsilon_{\text{ef}} = 27\%$ and the equation, $[\text{CO}_{2\text{aq}}] = (4.14[\text{PO}_4^{3-}]^2 + 125.48[\text{PO}_4^{3-}] + 107.85)/(27 - \varepsilon_{\text{p}})$. Minimum $[\text{CO}_{2\text{aq}}]$ calculated using an $\varepsilon_{\text{f}} = 25\%$ and the equation, $[\text{CO}_{2\text{aq}}] = (116.12[\text{PO}_4^{3-}] + 81.5)/(25 - \varepsilon_{\text{p}})$. Haptophyte production depths and seasonal phosphate concentrations were established using seasonal phosphate–temperature–depth relationships established by NOPACCS and U_{37}^K temperature values. Pre-industrial, water-column $[\text{CO}_{2\text{aq}}]$ were estimated by removing anthropogenic $[\text{CO}_{2\text{aq}}]$ from modern $[\text{CO}_{2\text{aq}}]$. The concentration of anthropogenic $\text{CO}_{2\text{aq}}$ at each site was simulated from a modified version of the Geophysical Fluid Dynamics Laboratory’s Modular Ocean Model (Duffy & Caldeira 1997; Pacanowski *et al.* 1991).

600 ppmv), where the C_4 photosynthetic pathway is favoured over C_3 photosynthesis. However, pCO_2 estimates lend no support to this supposition (Pagani *et al.* 1999b) (figure 13).

An interval of global warmth returns in the early to middle Pliocene. Maximum temperatures were established by *ca.* 3 Ma with high-latitude North Atlantic temperatures as much as 6 °C higher than today (Dowsett & Poore 1991; Cronin 1991). Global cooling followed the moderate climate of the middle Pliocene as major ice-sheet expansion in the Northern Hemisphere occurred between 3.1 and 2.5 Ma (Shackleton *et al.* 1984; Tiedemann *et al.* 1994).

Low pCO_2 over the past 25 Myr has important implications for climate research. First, if alkenone-based CO_2 estimates are valid, then modern levels are higher than

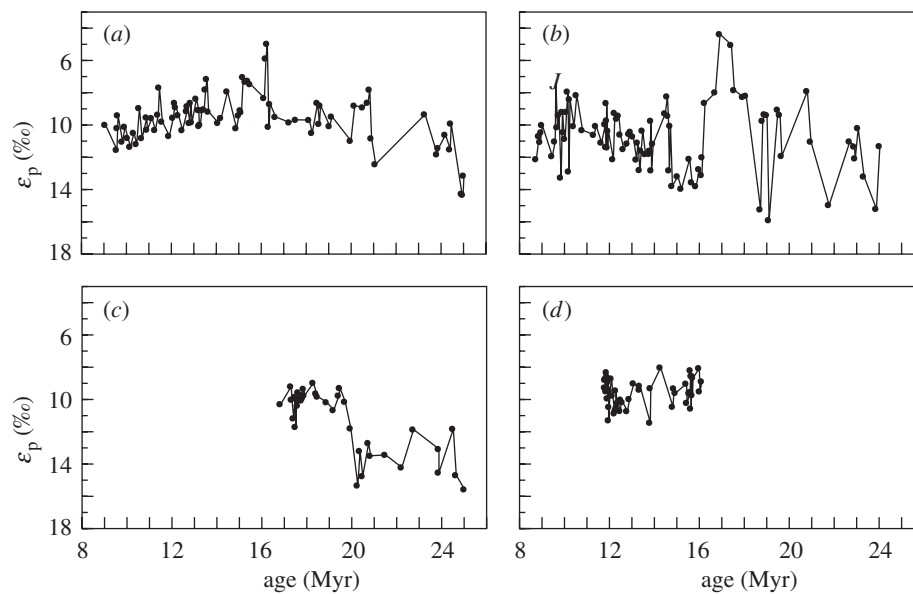


Figure 10. Miocene alkenone-based ε_p records from Deep Sea Drilling Project (DSDP) (a) Site 588 (Southwest Pacific), (b) Site 608 (North Atlantic), (c) Site 516 (Southwest Atlantic), and (d) Ocean Drilling Program (ODP) Site 730 (North Indian, Oman margin) (Pagani *et al.* 1999a).

they have been for at least the past 25 Myr. This suggests that the history of Neogene climate is inadequate as a reference for future changes in climate as CO_2 continues to rise. In addition, if one assumes that pCO_2 is the principal driver of Neogene climate, it is difficult to reconcile large-scale variations in temperatures, ice-volume and ecology with apparently small fluctuations in atmospheric carbon dioxide. Rather, it appears that other factors such as tectonically induced changes in ocean circulation and orogenesis were critical agents of climate change during this time (Pagani *et al.* 1999a, b). The opening of the Drake Passage, subsidence of the Greenland–Scotland Ridge, the restriction of flow across the Indian Ocean, cessation of flow through the eastern and western Mediterranean Sea, and the closure of the Panamanian Isthmus would have substantially altered ocean circulation, forcing changes in the hydrologic cycle and ocean heat transport. It is probable that the climatic effects of these processes were amplified under low levels of atmospheric carbon dioxide. Indeed, one would anticipate that the character of global climates would remain relatively stable and buffered from change under extreme greenhouse conditions, whereas under a low CO_2 atmosphere, Earth's climates are likely to be more sensitive and responsive to changes in physical oceanography and mountain-building events.

Although the ability to accurately reconstruct Holocene water-column CO_2 is encouraging and supports the efficacy of the alkenone approach for core-top sediments (figure 9), the underlying assumptions applied in more ancient CO_2 research are difficult, if not impossible, to verify. As previously discussed, these assumptions include the long-term endurance of a diffusive model of carbon uptake, the *b*-phosphate–micronutrient relationship, and algal cell geometries. One could argue that alkenone-producing algal physiologies, and their carbon isotopic compositions, evolved in close association with the evolution of climate and, thus, account for con-

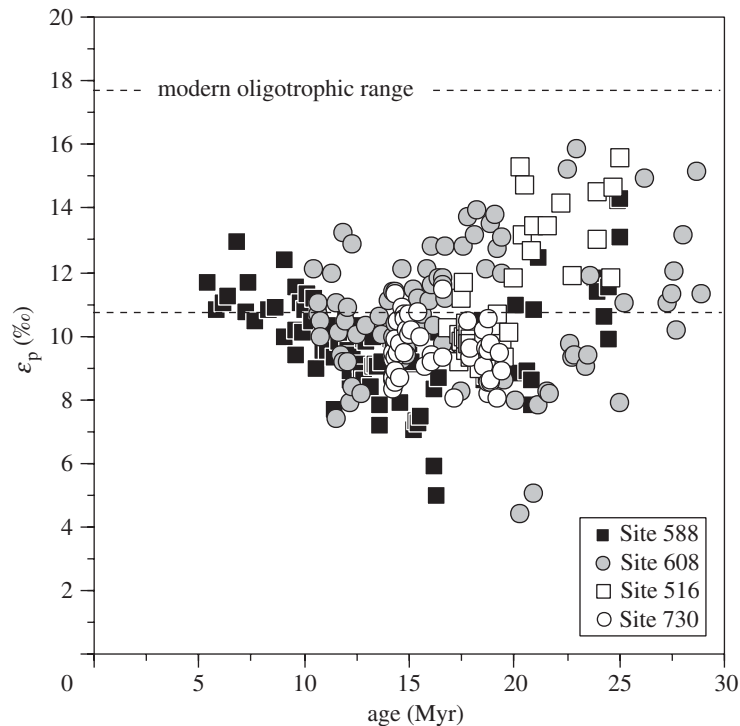


Figure 11. Comparison of Miocene ε_p values with the range of ε_p values from modern, oligotrophic environments. Modern data from Bidigare *et al.* (1997), Popp *et al.* (1999), Eek *et al.* (1999) and Laws *et al.* (2000).

sistently low Neogene ε_p values. Such arguments are warranted given the apparent ability of some extant haptophytes to actively transport inorganic carbon (Burns & Beardall 1987; Raven & Johnston 1991), and/or use carbonic anhydrase (Quiroga & Gonzalez 1993; Nimer *et al.* 1994), an enzyme that catalyses the reversible hydration of carbon dioxide (Tsuzuki & Miyachi 1989). The long-term selection of carbon concentrating mechanisms (CCMs) would clearly affect alkenone carbon isotopic compositions and distort CO₂ estimates. However, their prevalence would imply carbon limitation in Miocene oligotrophic environments and thus also support low surface-water CO₂ concentrations. Further, it is unlikely that the selection of an energetically expensive CCM would be widespread under high pCO₂.

Other considerations, such as secular changes in the *b*-phosphate–micronutrient relationship and algal cell geometries, are difficult to prove, but could account for low Miocene ε_p values under high-CO₂ conditions.

(b) Palaeogene records

An effort to extend alkenone-based ε_p records into the Palaeogene is ongoing and preliminary results appear to alleviate some of the concerns discussed above. The first phase of this work is focused on the Eocene/Oligocene (E/O) transition, which represents a critical climatic step away from the pervasive warmth of the Eocene (Zachos *et al.* 1994). Rapid and severe changes occurred at the E/O boundary, with the deep ocean cooling *ca.* 4 °C in less than 350 kyr (Zachos *et al.* 1996) in association

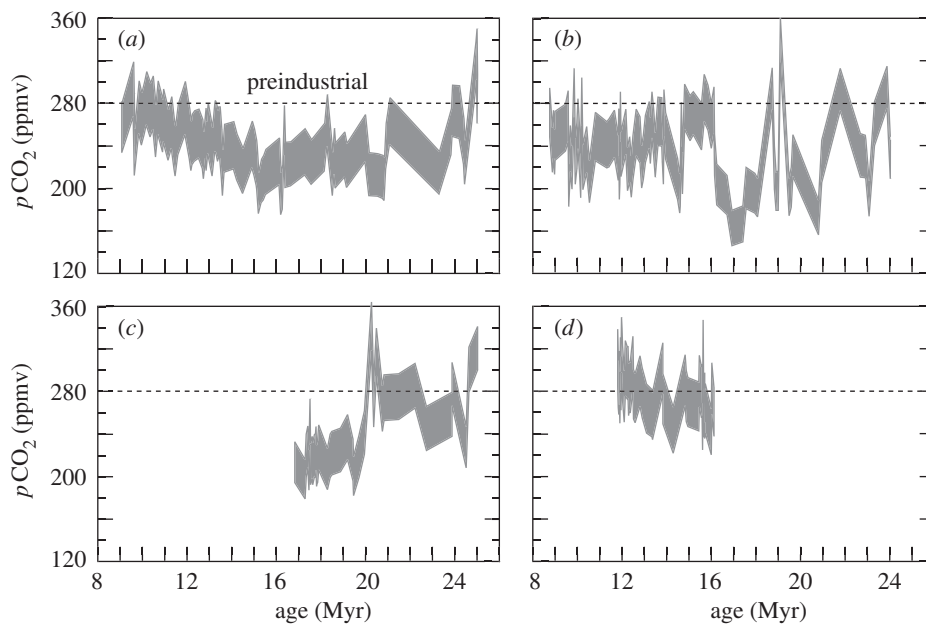


Figure 12. Maximum $p\text{CO}_2$ estimates calculated from ε_p records shown in figure 12. $[\text{CO}_{2\text{aq}}]$ derived by applying a range of values for ε_f (25–27‰). $p\text{CO}_2$ calculated from $[\text{CO}_{2\text{aq}}]$ by applying Henry's law and temperatures derived from coeval planktic foraminifera $\delta^{18}\text{O}$ (Pagani *et al.* 1999a). $p\text{CO}_2$ values represented by the right edge of the shaded band are calculated using a value of 27‰ for ε_f , $[\text{PO}_4^{3-}] = 0.3 \mu\text{mol l}^{-1}$, and an equation for the physiological-dependent term b calculated using the upper 95% confidence limit from the global dataset derived from all available data ($b_{(27\text{‰})} = 4.14[\text{PO}_4^{3-}]^2 + 125.48[\text{PO}_4^{3-}] + 107.85$). Values on the left edge of the shaded band are calculated using a value of 25‰ for ε_f , $[\text{PO}_4^{3-}] = 0.2 \mu\text{mol l}^{-1}$, and an equation for the physiological-dependent term b calculated using the geometric mean regression from the global dataset ($b_{(25\text{‰})} = 116.12[\text{PO}_4^{3-}] + 81.5$). ((a) Site 588, Southwest Pacific; (b) Site 608, North Atlantic; (c) Site 516, Southwest Atlantic; and (d) Site 730, Northwest Indian.)

with a massive expansion of continental ice sheets on Antarctica (Robert & Kennett 1997). Although episodic glaciations are apparent during the late Eocene (Browning *et al.* 1996), the E/O transition represents Earth's first clear step into the 'icehouse' conditions of the Cenozoic.

Alkenone $\delta^{13}\text{C}$ values were measured at the E/O boundary from two ocean sites (DSDP Sites 277 and 516) encompassing a range of growth environments (figure 14a). Compared with modern and Miocene data, E/O $\delta^{13}\text{C}$ values are considerably lower, providing evidence that ancient alkenone $\delta^{13}\text{C}$ values can indeed be much more depleted in ^{13}C than Miocene or modern values.

While it is clear that growth rate and CO_2 exert considerable influence on alkenone $\delta^{13}\text{C}$, variability in ε_p in the modern ocean appears to be primarily a function of $[\text{PO}_4^{3-}]$ and not $[\text{CO}_{2\text{aq}}]$ (figure 6). This suggests that while the modern range of ε_p is controlled by differences in haptophyte growth rates, the maximum and minimum limits of variability are dictated by the present range of surface-water $[\text{CO}_{2\text{aq}}]$. It follows that if $[\text{CO}_{2\text{aq}}]$ was higher during the Palaeogene, the limits of ε_p would be shifted toward higher values relative to the modern. Therefore, these results provide

Table 1. *DSDP Site 588*

(Data from M. Pagani, K. H. Freeman & M. A. Arthur (2002, unpublished data); 'NA' denotes 'not available'.)

age (Ma)	$\delta^{13}\text{C}_{\text{alk}}$	ε_{p}
0.008	-24.25	12.05
0.111	-23.27	10.14
0.216	-23.52	10.52
0.235	-23.38	10.29
0.369	-23.49	10.65
0.416	-23.57	NA
0.572	-23.08	9.91
1.471	-23.51	10.55
1.611	-21.76	8.89
1.890	-23.15	10.53
3.691	-23.11	10.93
3.557	-23.85	11.43
4.050	-22.77	10.61
4.185	-23.49	11.13
4.310	-23.26	11.17
4.571	-23.55	11.19
4.859	-23.33	11.02
5.069	-23.25	11.18
5.243	-22.88	10.86
5.322	-23.45	11.05

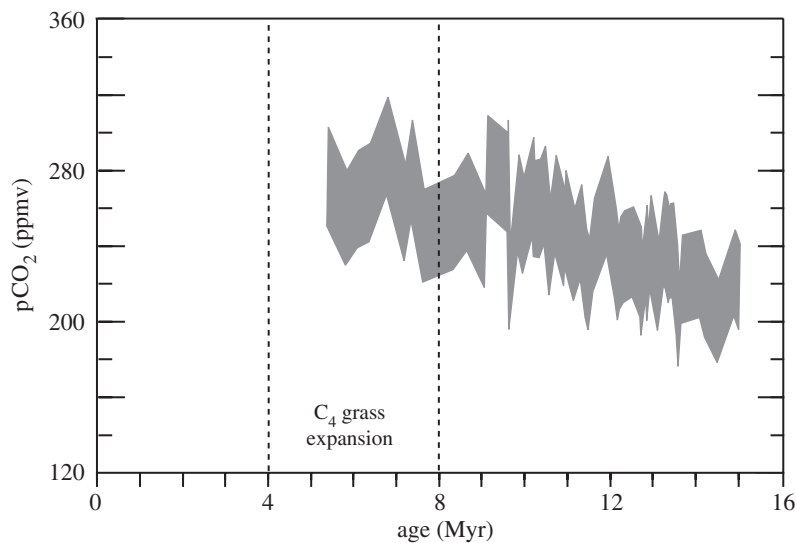


Figure 13. Late Miocene pCO₂ estimates from Site 588 in relation to the expansion of C₄ grasses (from Pagani *et al.* 1999b). See the caption for figure 12 for equations and variables used to calculate pCO₂.

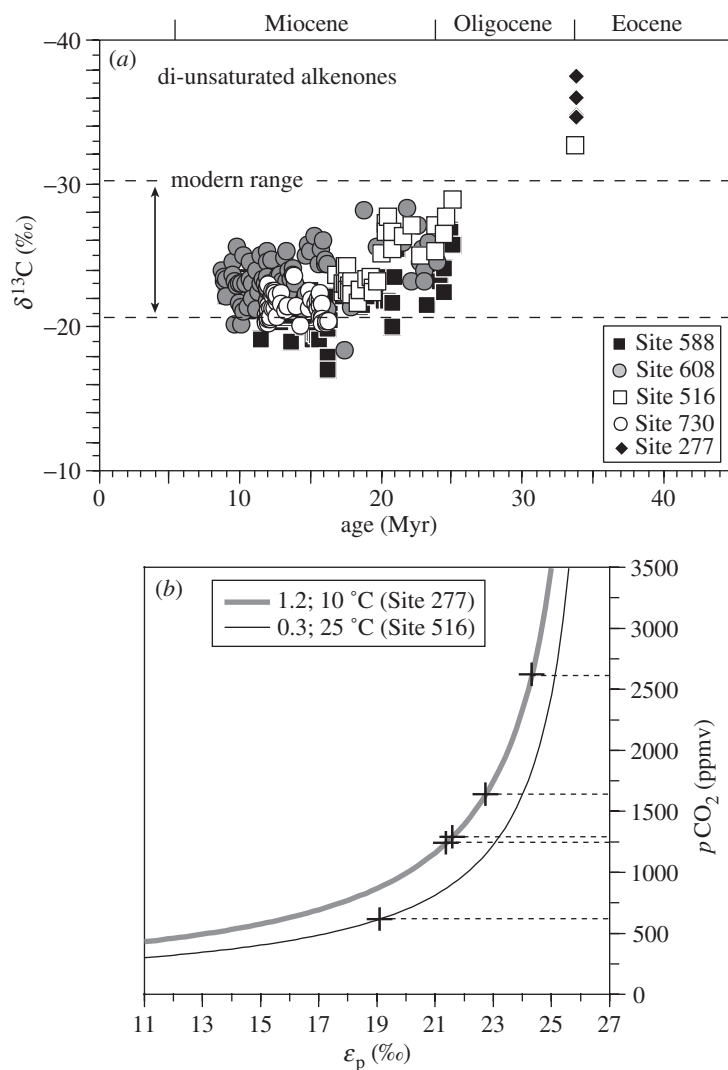


Figure 14. (a) Compilation of $\delta^{13}\text{C}$ values of sedimentary diunsaturated alkenones. The dashed lines capture the range of alkenone values collected from water-column samples (E/O values from M. Pagani, J. C. Zachos & K. H. Freeman 2002, unpublished data). (b) Estimates of Eocene/Oligocene $p\text{CO}_2$. Values from Site 277 are estimated using the equation $[\text{CO}_{2\text{aq}}] = (128.96[\text{PO}_4^{3-}] + 101.37)/(27 - \epsilon_p)$, $[\text{PO}_4^{3-}] = 1.6 \mu\text{mol l}^{-1}$, temperature = 10 °C. Values from Site 516 are estimated using $[\text{PO}_4^{3-}] = 0.3 \mu\text{mol l}^{-1}$, temperature = 25 °C. E/O values are not in stratigraphic order.

preliminary evidence for higher $p\text{CO}_2$ conditions at the E/O boundary relative to the present.

Carbon dioxide concentrations can be estimated from these data if we apply the modern b versus phosphate relationship, reasonable $[\text{PO}_4^{3-}]$, and further assume that the $\delta^{13}\text{C}$ of $\text{CO}_{2\text{aq}}$ at each site was -10‰ (relatively negative compared with modern values). Using these assumptions, *minimum* estimates of $p\text{CO}_2$ calculated from these

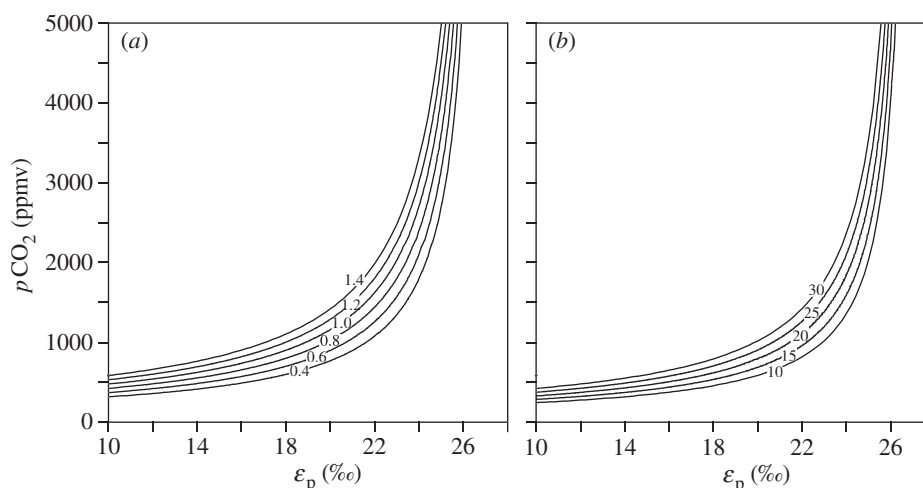


Figure 15. Plot of ε_p versus $p\text{CO}_2$. (a) Contours are $[\text{PO}_4^{3-}]$ ($\mu\text{mol l}^{-1}$), $p\text{CO}_2$ calculated at 22 °C. (b) Contours are temperature (°C), $[\text{CO}_{2\text{aq}}]$ calculated using $[\text{PO}_4^{3-}] = 0.3 \mu\text{mol l}^{-1}$.

data suggest that carbon dioxide concentrations were *ca.* 2–5 times (and perhaps higher) than modern levels (figure 14b).

As ε_p approaches maximum theoretical values (equivalent to ε_f), the potential error in calculated $p\text{CO}_2$ increases markedly (figure 15a). Analytical uncertainty (*ca.* $\pm 0.4\%$) alone is responsible for 200–300 ppmv uncertainty for a ε_p value of 23‰. Furthermore, temperature-dependent errors will tend to increase in older sequences due to the difficulty in reconstructing accurate sea-surface temperatures from foraminifera $\delta^{18}\text{O}$ (figure 15b). Finally, low E/O alkenone $\delta^{13}\text{C}$ values could result from extreme differences in cellular geometries of alkenone-producing algae relative to the present. Such differences are difficult to quantify, but a qualitative assessment could be approached through future analyses of coccolith morphologies.

These uncertainties highlight the importance of developing ancient alkenone-based CO₂ records using multiple ocean localities and extensive data collection. Therefore, given the paucity of data collected to date, the results presented for the E/O boundary should be cautiously applied.

5. Conclusions

Alkenones are distinct molecular markers derived from limited species of haptophyte microalgae in the modern ocean, and to the best of our knowledge, were produced by similar organisms in the geological past. Culture experiments performed on alkenone-producing organisms are limited, but show a distinct relationship between cellular growth rate, carbon dioxide concentration, and the total stable carbon isotope fractionation that occurs during photosynthesis (ε_p). Furthermore, extensive field measurements have unveiled a significant correlation between the concentration of soluble phosphate and ε_p . This chemical–physiological association has provided a mathematical relationship that allows for the calculation of ancient $[\text{CO}_{2\text{aq}}]$ if values of ε_p are known and phosphate concentrations are reasonably constrained. As is the case with all CO₂ proxies, the validity of ancient $p\text{CO}_2$ records is only as robust as the validity of the underlying assumptions of the technique. Although the alkenone

approach is demonstrably accurate in the reconstruction of Holocene water-column [$\text{CO}_{2\text{aq}}$], the integrity of similar assumptions in more ancient sediments is difficult to confirm. Thus, unravelling the history of atmospheric carbon dioxide will ultimately require relative agreement of pCO_2 records derived from disparate approaches.

The available data suggest that ancient alkenone-based ε_p values encompass a broad range. Low ε_p values, similar to and lower than today's, characterize sediments encompassing the past 25 Myr, whereas much higher values have recently been recorded across the Eocene/Oligocene boundary. If the temporal expression of these records results from the evolution of carbon dioxide concentrations, and not algal physiologies, then it suggests that pCO_2 was at least 2–5 times higher at the end of the Eocene and declined to near modern levels by the beginning of the Miocene.

This manuscript was improved by helpful reviews from R. Pancost and R. Schneider, and conversations with B. Popp.

References

- Andersen, N., Müller, P. J., Kirst, G. & Schneider, R. R. 1999 The $\delta^{13}\text{C}$ signal in $\text{C}_{37:2}$ alkenones as a proxy for reconstructing Late Quaternary pCO_2 in surface waters from the South Atlantic. In *Proxies in paleoceanography: examples from the South Atlantic* (ed. G. Fischer & G. Wefer), pp. 469–488. Springer.
- Arthur, M. A., Walter, D. E. & Claypool, G. E. 1985 Anomalous ^{13}C enrichment in modern marine organic carbon. *Nature* **315**, 216–218.
- Arthur, M. A., Hinga, K. R., Pilson, M. E. Q., Whitaker, E. & Allard, D. 1991 Estimates of pCO_2 for the last 120 Ma based on the $\delta^{13}\text{C}$ of marine phytoplanktic organic matter. *Eos* **72**, 166.
- Berner, R. A. (and 10 others) 2000 Isotope fractionation and atmospheric oxygen: implications for Phanerozoic O_2 evolution. *Science* **287**, 1630–1633.
- Berner, R. & Kothavala, Z. 2001 GEOCARB III: a revised model of atmospheric CO_2 over Phanerozoic Time. *Am. J. Sci.* **301**, 182–204.
- Bidigare, R. R. (and 14 others) 1997 Consistent fractionation of ^{13}C in nature and in the laboratory: growth-rate effects in some haptophyte algae. *Global Biogeochem. Cycles* **11**, 279–292.
- Bidigare, R. R. (and 14 others) 1999 Correction to 'Consistent fractionation of ^{13}C in nature and in the laboratory: growth-rate effects in some haptophyte algae' by Bidigare *et al.* 1997. *Global Biogeochem. Cycles* **13**, 251.
- Brassell, S. C., Eglinton, G., Marlowe, I. T., Pflaumann, U. & Sarnthein, M. 1986 Molecular stratigraphy: a new tool for climatic assessment. *Nature* **320**, 129–133.
- Browning, J. V., Miller, K. G. & Pak, D. K. 1996 Global implications of lower to middle Eocene sequence boundaries on the New Jersey coastal plain: the icehouse cometh. *Geology* **24**, 639–642.
- Burkhardt, S., Riebesell, U. & Zondervan, I. 1999 Effects of growth rate, CO_2 concentration, and cell size on the carbon isotope fraction in marine phytoplankton. *Geochim. Cosmochim. Acta* **63**, 3729–3741.
- Burns, B. D. & Beardall, J. 1987 Utilization of inorganic carbon by marine microalgae. *J. Exp. Mar. Ecol.* **107**, 75–86.
- Cerling, T. E., Harris, J. M., MacFadden, B. J., Leakey, M. G., Quade, J., Eisenmann, V. & Ehleringer, J. R. 1997 Global vegetation change through the Miocene/Pliocene boundary. *Nature* **389**, 153–158.

- Compton, J. S., Snyder, S. W. & Hodell, D. A. 1990 Phosphogenesis and weathering of shelf sediments from the southeastern United States: implications for Miocene $\delta^{13}\text{C}$ excursions and global cooling. *Geology* **18**, 1227–1230.
- Conte, M. H., Volkman, J. K. & Eglinton, G. 1994 Lipid biomarkers of the Haptophyta. In *The Haptophyte algae* (ed. J. C. Green & B. S. C. Leadbeater), pp. 351–377. Clarendon.
- Cronin, T. M. 1991 Pliocene shallow water paleoceanography of the North Atlantic ocean based on marine ostracodes. *Quat. Sci. Rev.* **10**, 175–188.
- Degens, E. T., Guillard, R. R. L., Sackett, W. M. & Hellebust, J. A. 1968 Metabolic fractionation of carbon isotopes in marine plankton. I. Temperature and respiration experiments. *Deep Sea Res. I* **15**, 1–9.
- Dowsett, H. J. & Poore, R. Z. 1991 Pliocene sea surface temperatures of the North Atlantic at 3.0 Ma. *Quat. Sci. Rev.* **10**, 189–204.
- Duffy, P. B. & Caldeira, K. 1997 Sensitivity of simulated salinity in a three-dimensional ocean model to upper ocean transport of salt from sea-ice formation. *Geophys. Res. Lett.* **24**, 1323–1326.
- Eek, M. E., Whitticar, M. J., Bishops, J. K. B. & Wong, C. S. 1999 Influence of nutrients on carbon isotope fractionation by natural populations of Pymnesiophyte algae in NE Pacific. *Deep Sea Res. II* **46**, 2863–2876.
- Falkowski, P. G. 1991 Species variability in the fractionation of ^{13}C and ^{12}C by marine phytoplankton. *J. Plankton Res.* **13** (Supplement), 21–28.
- Farquhar, G. D. & Richards, P. A. 1984 Isotopic composition of plant carbon correlates with water-use efficiency of wheat genotypes. *Aust. J. Plant Physiol.* **11**, 539–552.
- Farquhar, G. D., O’Leary, M. H. & Berry, J. A. 1982 On the relationship between carbon isotope discrimination and the intercellular carbon dioxide concentration in leaves. *Aust. J. Plant Physiol.* **13**, 281–292.
- Farrimond, P., Eglinton, G. & Brassell, S. C. 1986 Alkenones in Cretaceous black shales, Blake-Bahama Basin, western North Atlantic. **10**, 897–903.
- Flower, B. P. & Kennett, J. P. 1993 Middle Miocene ocean-climate transition: high-resolution oxygen and carbon isotopic records from Deep Sea Drilling Project Site 588A, Southwest Pacific. *Paleoceanography* **8**, 811–843.
- Francois, R., Altabet, M. A., Goericke, R., McCorkle, D. C., Brunet, C. & Poisson, A. 1993 Changes in the $\delta^{13}\text{C}$ of surface water particulate organic matter across the subtropical convergence in the SW Indian Ocean. *Global Biogeochem. Cycles* **7**, 627–644.
- Freeman, K. H. & Hayes, J. M. 1992 Fractionation of carbon isotopes by phytoplankton and estimates of ancient CO₂ levels. *Global Biogeochem. Cycles* **6**, 185–198.
- Freeman, K. H., Hayes, J. M., Trendel, J. & Albrecht, P. 1990 Evidence from carbon isotope measurements for diverse origins of sedimentary hydrocarbons. *Nature* **343**, 254–256.
- Goericke, R., Montoya, J. P. & Fry, B. 1994 Physiology of isotope fractionation in algae and cyanobacteria. In *Stable isotope in ecology* (ed. K. Lajtha & B. Michener), Cambridge: Blackwell Scientific.
- Hay, W. W. 1977 Calcareous nannofossils. In *Oceanic micropaleontology* (ed. A. T. S. Ramsay), pp. 1055–1200. Academic.
- Hayes, J. M., Freeman, K. H., Popp, B. N. & Homan, C. H. 1990 Compound-specific isotopic analyses: a novel tool for reconstruction of ancient biogeochemical processes. *Org. Geochem.* **16**, 1115–1128.
- Jasper, J. P., Mix, A. C., Prahl, F. G. & Hayes, J. M. 1994 Photosynthetic fractionation of ^{13}C and concentrations of dissolved CO₂ in the central equatorial Pacific during the last 255,000 years. *Paleoceanography* **6**, 781–798.
- Jasper, J. P. & Hayes, J. M. 1990 A carbon isotope record of CO₂ levels during the Late Quaternary. *Nature* **347**, 462–464.

- Keigwin, L. 1982 Isotopic paleoceanography of the Caribbean and East Pacific: role of Panama uplift in late Neogene time. *Science* **217**, 350–353.
- Kennett, J. P. 1977 Cenozoic evolution of Antarctic glaciation, the circum-Antarctic Ocean, and their impact on global paleoceanography. *J. Geophys. Res.* **82**, 3843–3860.
- Kroopnick, P. 1985 The distribution of ^{13}C of ΣCO_2 in the world oceans. *Deep Sea Res. I* **32**, 57–84.
- Laws, E. A., Popp, B. N., Bidigare, R. R., Kennicut, M. C. & Macko, S. A. 1995 Dependence of phytoplankton carbon isotopic composition on growth rate and $[\text{CO}_2]_{\text{aq}}$: theoretical considerations and experimental results. *Geochim. Cosmochim. Acta* **59**, 1131–1138.
- Laws, E. A., Bidigare, R. R. & Popp, B. N. 1997 Effect of growth rate and CO_2 concentration on carbon isotopic fractionation by the marine diatom *Phaeodactylum tricornutum*. *Limnol. Oceanogr.* **42**, 1552–1560.
- Laws, E. A., Popp, B. N. & Bidigare, R. R. 2000 Controls on the molecular distribution and carbon isotopic composition of alkenones in certain haptophyte algae. *Geochem. Geophys. Geosyst.* **2**, 2000GC000057.
- Lynch-Stieglitz, J., Stocker, T. F., Broecker, W. S. & Fairbanks, R. G. 1995 The influence of air–sea exchange on the isotopic composition of oceanic carbon: observations and modeling. *Global Geochem. Cycles* **9**, 653–665.
- McIntyre, A. 1970 *Gephyrocapsa protohuxleyi* sp. n., a possible phyletic link and index fossil for the Pleistocene. *Deep Sea Res. I* **17**, 187–190.
- Marlowe, I. T., Brassell, S. C., Eglinton, G. & Green, J. C. 1990 Long-chain alkenones and alkyl alkenones and the fossil coccolith records of marine sediments. *Chem. Geol.* **88**, 349–375.
- Merritt, D. A., Freeman, K. H., Ricci, M. P., Studley, S. S. & Hayes, J. M. 1995 Performance and optimization of a combustion interface for isotope ratio monitoring gas chromatography/mass spectrometry. *Analyt. Chem.* **67**, 2461–2473.
- Miller, K. G., Fairbanks, R. G. & Mountain, G. S. 1987 Tertiary oxygen isotope synthesis, sea level history, and continental margin erosion. *Paleoceanography* **2**, 1–19.
- Nimer, N. A., Guan, Q. & Merrett, M. J. 1994 Extra- and intra-cellular carbonic anhydrase in relation to culture strain of *Emiliana huxleyi* Lohmann. *New Phytologist* **126**, 601–607.
- Ohkouchi, N., Kawamura, K., Kawahata, H. & Okada, H. 1999 Depth ranges of alkenone production in the Central Pacific Ocean. *Global Biogeochem. Cycles* **13**, 695–704.
- Pacanowski, R., Dixon, K. & Rosati, A. 1991. The G.F.D.L. Modular Ocean Model Users Guide version 1.0. NOAA/Geophysical Fluid Dynamics Laboratory, Princeton, NJ.
- Pagani, M., Arthur, M. A. & Freeman, K. H. 1999a The Miocene evolution of atmospheric carbon dioxide. *Paleoceanography* **14**, 273–292.
- Pagani, M., Freeman, K. H. & Arthur, M. A. 1999b Late Miocene CO_2 concentrations and the expansion of C_4 grasses. *Science* **285**, 876–879.
- Pagani, M., Arthur, M. A. & Freeman, K. H. 2000a Variations in Miocene phytoplankton growth rates in the Southwest Atlantic: evidence for changes in ocean circulation. *Paleoceanography* **15**, 486–496.
- Pagani, M., Freeman, K. H. & Arthur, M. A. 2000b Isotope analyses of molecular and total organic carbon from Miocene sediments. *Geochim. Cosmochim. Acta* **64**, 37–49.
- Pagani, M., Freeman, K. H., Ohkouchi, N. & Caldeira, K. 2002 A comparison of water column $[\text{CO}_{2\text{aq}}]$ with sedimentary alkenone-based estimates: a test of the paleo- pCO_2 proxy. (Submitted.)
- Pearson, P. N. & Palmer, M. R. 2000 Atmospheric carbon dioxide concentrations over the past 60 million years. *Nature* **406**, 695–699.
- Popp, B. N., Laws, E. A., Bidigare, R. R., Dore, J. E., Hanson, K. L. & Wakeham, S. G. 1998 Effect of phytoplankton cell geometry on carbon isotopic fractionation. *Geochim. Cosmochim. Acta* **62**, 69–77.

- Popp, B. N., Hanson, K. L., Dore, J. E., Bidigare, R. R., Laws, E. A. & Wakeham, S. G. 1999 Controls on the carbon isotopic composition of phytoplankton: paleoceanographic perspectives. In *Reconstructing ocean history: a window into the future* (ed. F. Abrantes & A. Mix). New York: Plenum.
- Quiroga, O. & Gonzalez, E. 1993 Carbonic anhydrase in the chloroplast of a coccolithophorid (Prymnesiohycea). *J. Phycol.* **29**, 321–324.
- Rau, G. H., Takahashi, T. & Des Marais, D. J. 1989 Latitudinal variations in plankton $\delta^{13}\text{C}$: implications for CO₂ and productivity in past oceans. *Nature* **341**, 516–518.
- Rau, G. H., Takahashi, T., Des Marais, D. J., Repeta, D. J. & Martin, J. H. 1992 The relationship between $\delta^{13}\text{C}$ of organic matter and [CO₂(aq)] in ocean surface water: data from a JGOFS site in the Northeast Atlantic Ocean and a model. *Geochim. Cosmochim. Acta* **56**, 1413–1419.
- Raven, J. A. & Johnston, A. M. 1991 Mechanisms of inorganic-carbon acquisition in marine phytoplankton and their implications for the use of other resources. *Limnol. Oceanogr.* **36**, 1701–1714.
- Raymo, M. E. 1994 The Himalayas, organic carbon burial, and climate in the Miocene. *Paleoceanography* **9**, 399–404.
- Raymo, M. E., Ruddiman, W. F. & Froelich, P. N. 1988 Influence of late Cenozoic mountain building on ocean geochemical cycles. *Geology* **16**, 649–653.
- Rechka, J. A. & Maxwell, J. R. 1987 Characterisation of alkenone temperature indicators in sediments and organisms. *Org. Geochem.* **13**, 727–734.
- Riebesell, U., Revill, A. T., Hodsworth, D. G. & Volkman, J. K. 2000 The effects of varying CO₂ concentration on lipid composition and carbon isotope fractionation in *Emiliania huxleyi*. *Geochim. Cosmochim. Acta* **64**, 4179–4192.
- Robert, C. & Kennett, J. P. 1997 Antarctic continental weathering changes during Eocene–Oligocene cryosphere expansion: clay mineral and oxygen isotope evidence. *Geology* **25**, 587–590.
- Roeske, C. A. & O’Leary, M. H. 1984 Carbon isotope effect in the enzyme-catalyzed carboxylation of ribulose biphosphate. *Biochemistry* **23**, 6275–6285.
- Royer, D. L., Wing, S. L., Beerling, D. J., Jolley, D. W., Koch, P. L., Hickey, L. J. & Berner, R. A. 2001 Paleobotanical evidence for near present-day levels of atmospheric CO₂ during part of the Tertiary. *Nature* **292**, 2310–2313.
- Ruddiman, W. F., Prell, W. L. & Raymo, M. E. 1989 Late Cenozoic uplift in southern Asia and the American West: rationale for general circulation modeling experiments. *J. Geophys. Res.* **94**, 18409–18427.
- Ruddiman, W. F., Kutzbach, J. E. & Prentice, I. C. 1997 Testing the climatic effects of orography and CO₂ with general circulation and biome models. In *Tectonic uplift and climate change* (ed. W. F. Ruddiman), pp. 204–235. New York: Plenum.
- Savin, S. M., Douglas, R. G. & Stehli, F. G. 1975 Tertiary marine paleotemperatures. *Geol. Soc. Am. Bull.* **86**, 1499–1510.
- Shackleton, N. J. (and 16 others) 1984 Oxygen isotope calibration of the onset of ice-rafting and history of glaciation in the North Atlantic region. *Nature* **307**, 620–623.
- Shackleton, N. J. & Kennett, J. P. 1975 Paleotemperature history of the Cenozoic and the initiation of Antarctic glaciation: oxygen and carbon isotope analyses in DSDP Sites 277, 279, and 281. *Init. Rep. Deep Sea Drill. Proj.* **29**, 743–755.
- Sharkey, T. D. & Berry, J. A. 1985 Carbon isotope fractionation of algae as influenced by an inducible CO₂ concentration mechanism. In *Inorganic carbon uptake by aquatic photosynthetic organisms* (ed. W. J. Lucas & J. A. Berry), pp. 389–401. American Society of Plant Physiologists.
- Tiedemann, R., Sarnthein, M. & Shackleton, N. J. 1994 Astronomical calibration for Pliocene Atlantic $\delta^{18}\text{O}$ and dust flux records of Ocean Drilling Program Site 659. *Paleoceanography* **9**, 619–638.

- Tsubota, H., Ishizaka, J., Nishimura, A. & Watanabe, Y. W. 1999 Overview of NOPACCS (Northwest Pacific Carbon Cycle Study). *J. Oceanogr.* **55**, 645–653.
- Tsuzuki, M. & Miyachi, S. 1989 The function of carbonic anhydrase in aquatic photosynthesis. *Aquat. Bot.* **34**, 85–104.
- van der Burg, J., Visscher, H., Dilcher, D. L. & Kürschner, W. M. 1993 Paleoatmospheric signatures in Neogene fossil leaves. *Science* **260**, 1788–1790.
- Verity, P. G., Robertson, C. Y., Tronzo, C. R., Andrews, M. G., Nelson, J. R. & Sieracki, M. E. 1993 Relationships between cell volume and the carbon and nitrogen content of marine photosynthetic nanoplankton. *Limnol. Oceanogr.* **37**, 1434–1446.
- Vincent, E. & Berger, W. H. 1985 Carbon dioxide and polar cooling in the Miocene: the Monterey hypothesis. In *The carbon cycle and atmospheric CO₂: natural variations from the Archean to present* (ed. E. T. Sundquist & W. S. Broecker), pp. 455–468. Washington, DC: American Geophysical Union.
- Volkman, J. K. 2000 Ecological and environmental factors affecting alkenone distributions in seawater and sediments. *Geochem. Geophys. Geosyst.* **1**, 2000GC000061.
- Wong, W. W. & Sackett, W. M. 1978 Fractionation of stable carbon isotopes by marine phytoplankton. *Geochim. Cosmochim. Acta* **42**, 1809–1815.
- Wright, J. D., Miller, K. G. & Fairbanks, R. G. 1992 Early and middle Miocene stable isotopes: implications for deepwater circulation and climate. *Paleoceanography* **7**, 357–389.
- Zachos, J. C., Stott, L. D. & Lohmann, K. C. 1994 Evolution of early Cenozoic marine temperatures. *Paleoceanography* **9**, 353–387.
- Zachos, J. C., Quinn, T. M. & Salamy, K. A. 1996 High-resolution (10⁴ years) deep-sea foraminiferal stable isotope records of the Eocene–Oligocene climate transition. *Paleoceanography* **11**, 251–266.